Influence of irregular geologies and inhomogeneity on SH-wave propagation

Rupinderjit Kaur[1*] , Sumit Kumar Vishwakarma[1], Tapas Ranjan Panigrahi[1]

[1]Department of Mathematics, BITS-Pilani, Hyderabad Campus, Hyderabad-500078, India

[*] Corresponding author: kaurrupinderjit29@gmail.com

November 13, 2019

1 Abstract

In the present paper, the study has been performed in an irregular earth crust, layered over a semi-infinite half-space under the effect of gravity. The irregularities at the interface are possible combinations of geometric shapes such as rectangular, parabola and triangular notch. The aim of the study is to come up with the influence of these irregularities on the phase velocity of shear horizontal waves. The current work also indulges with the outcome as to how inhomogeneities leave a remarkable effect on SH-wave propagation. The medium has been assumed to exhibit inhomogeneities as the function of depth. These functions are the product of linear algebraic function and exponential function of depth. By means of separation of variables and substitution method, the equation of motion has been reduced to the Hypergeometric equation. Suitable boundary conditions have been employed to derive a closed form of dispersion equation. Numerical computations have been performed to visualize the impact of irregularity and inhomogeneity. It has been observed that irregular interfaces and inhomogeneity involved in the medium has a significant bearing on SH-wave propagation.

Keywords: Hypergeometric function, laguerre function, SH-wave, inhomogeneity, irregular interface.

2 Introduction

The materials which show viscous as well as elastic behavior while undergoing deformation are viscoelastic materials, have viscosity factor and time-dependent strain rate. Also, energy is dissipated as heat on applying a load on viscoelastic materials, therefore used for isolating vibration, reducing noise and absorbing shocks. From a geological point of view, the behavior of earth is assumed to be like an ideal elastic or viscoelastic material. Therefore, keeping in view the viscoelastic behavior of the layered earth, it is of great concern to study the propagation of SH-wave at an interface between an inhomogeneous viscoelastic layer and inhomogeneous gravitating half-space, which will have importance in solid mechanics, seismology and civil engineering.

Several studies have been done on the transmission of plane seismic waves in viscoelastic materials. Cooper [1] explained the transmission and reflection of plane shear waves at the interface of two linearly viscoelastic layers. Shaw presented a method for calculating stresses and displacements caused by a plane wave passing through a layered viscoelastic substratum and explained the fact that interface waves can exist in a viscoelastic layer under an elastic

half-space if the layer is pseudo-elastic [2]. Bhattacharya [3] provided a particular solution for SH-wave equation for a few inhomogeneities in terms of Bessel, Whittaker, Exponential and Hypergeometric functions. Schoenberg, Borcherdt, Lockett [4]–[6] explained the reflection and transmission of plane waves in layered inhomogeneous viscoelastic media. Whereas, Gogna [7] explained the propagation of SH-waves through an anisotropic inhomogeneous elastic half-space lying over viscoelastic half-space.Kanai explained the effect of solid viscosity of surface layer on earthquake movements [8].

In viscoelastic materials, slowness vector ($v = P + iA$) is complex-valued having P and A as propagation and attenuation vectors. The plane wave is called inhomogeneous for nonparallel propagation and attenuation vectors. Cerveny [9] discussed inhomogeneous harmonic waves in viscoelastic anisotropic media. She provided three approaches directional, componential and mixed specification to determine the slowness vector of an inhomogeneous plane wave in a viscoelastic medium. Wang [10] provided an analytical solution for phase velocity of body wave in an inhomogeneous transversely isotropic material whose Young's modulus, shear modulus and density vary according to the generalized power-law model $(\alpha + \beta z)^n$, where α and β are inhomogeneous parameters and coordinate z is along the depth of earth.

The boundaries of the earth's media are not regular because of mountain basins, mountain roots, ore bodies and rocky materials. The irregular surface of crustal layers of the earth affects the elastic wave propagation and plays a vital role in the energy distribution of reflected and refracted seismic waves. Therefore, it is of great concern to study the propagation of elastic waves at various types of imperfect interfaces of earth's media. Many authors have investigated seismic waves at irregular boundaries of earth's crustal layers. For example, Guoquan Nie [11] explained the propagation of SH-wave in piezoelectric–piezomagnetic bilayer system with an imperfect interface. Tomar [12] studied SH-waves at an irregular interface between a dry sandy half-space and an anisotropic elastic half-space. Chattopadhyay [13] investigated about reflection and refraction of plane quasi-P waves at a corrugated(imperfect) interface between distinct triclinic elastic half-spaces. Vishwakarma explained the torsional wave propagation in the earth's crustal layer under the influence of imperfect interface [14].

It was explained by Bullen [15] that the density inside the earth varies at different rates. He has also approximated the density law inside the earth varies quadratically (in-depth parameter) for 413 *Km* to 984 *Km* depth. Ongoing further towards the central core (> 984 *Km*), density varies as a linear function of depth parameter. Various attempts of variations for density inside earth such as linear, quadratic, harmonic as well as exponential have been made on the basis of Bullen's theory. For example, a hyperbolic variation of density has been taken by Sari and Salk [16]. Dey and Mukherjee [17] considered love waves in a granular medium over elastic half-space under hydrostatic initial stress due to gravity. Singh et al. [18] studied torsional surface wave propagation in a fiber composite layer lying over an initially stressed viscoelastic half-space. Sahu [19] investigated the propagation of SH-waves in a heterogeneous fiber-reinforced medium over a heterogeneous half-space under gravity. Chattopadhyay et al. [20] explained the propagation of shear waves in an irregular magnetoelastic monoclinic layer sandwiched between two isotropic half-spaces. He considered the irregularity in the surface as rectangular in shape. Vishwakarma et al. [21] studied the propagation of SH-wave in linearly varying fiber-reinforced viscoelastic composite structure under initial stress. Refernces may be given to Fang et al. [22] and Li et al. [23] in the field of SH-wave propagation.

The present paper attempts to study the possibility of SH-wave in an inhomogeneous visco-elastic layer over inhomogeneous half-space having different irregular interfaces. The materials inside the earth are anisotropic with elastic parameters that vary with orientation. Therefore, keeping in mind the anisotropy of the earth's crustal layer and the half-space, the rigidity and the viscosity has been taken as the product of a linear function and an exponential

function of depth, while density varies exponentially along with the depth. As the boundary of earth can never be flat throughout but are always irregular up to some extent. The roughness or irregular undulation of the boundary surface place an important role in the energy distribution of reflected and refracted waves. These irregular geologies or corrugated surfaces are made up of many geometrical shapes such as rectangular, parabolic and triangular notch. As the analytical treatment of irregularities of the surface entails formidable mathematical difficulties, we have considered possible combinations of the geometrical shapes i.e., Rectangle, parabola, triangular notch to come out with most promising irregular surface of different types. Method of separation of variables has been employed to derive the dispersion equation for the propagation of SH-wave. It has been observed that SH-wave transits in considered geometries. The graphical illustrations have been made to examine the effect of the various inhomogeneity parameters. Modelling SH-wave propagation in irregular geologies are helpful in forecasting geophysical parameters at greater depth through signal processing and seismic data modelling[24]. This study can also be applied to enhance our knowledge about the earth's structure.

3 Formation of Problem

We considered an inhomogeneous viscoelastic layer of finite thickness $\{H \le z \le sh(x)\}$ over an inhomogeneous half-space $\{sh(x) \le z < \infty\}$ with imperfect interface. The x-axis and the z-axis of co-ordinate system(x, y, z) have been taken along the direction of propagation of wave and towards the core of earth respectively. The origin O of the coordinate system has been taken such that imperfect interface is symmetrical about OZ. By keeping in mind the real scenario of earth, 6 kinds of imperfect interfaces of layer and half-space have been considered, and each imperfect interface is divided into two parts each of height H_1 and H_2 towards z-axis and have a span of length $2s$ on x-axis as shown in figure. These imperfect interfaces are a combination of the geometrical shapes rectangular, parabolic and triangular notch. The equation of imperfect interface is given by the function

$$z = s\,h(x) \tag{1}$$

The imperfect interfaces for 6 different geometries defined by $h(x)$ are given below and shown in figure (1).

$$h(x) = \begin{cases} 0, & s \le |x| \\ H_1, & \frac{s}{2} \le |x| \le s \\ H_1 + H_2\left(1 + \frac{2x}{s}\right), & -s \le x \le 0 \\ H_1 + H_2\left(1 - \frac{2x}{s}\right), & 0 \le x \le s \end{cases}$$

I

$$h(x) = \begin{cases} 0, & s \le |x| \\ \frac{2H_1}{s}(s - x), & \frac{s}{2} \le |x| \le s \\ \frac{2H_1}{s}(s + x), & -s \le x \le -\frac{s}{2} \\ H_1 + H_2, & -\frac{s}{2} < x < \frac{s}{2} \end{cases}$$

II

$$h(x) = \begin{cases} 0, & s \le |x| \\ H_1, & \frac{s}{2} \le |x| \le s \\ H_1 + H_2\left(1 - \frac{4x^2}{s^2}\right), & |x| \le \frac{s}{2} \end{cases}$$

III

$$h(x) = \begin{cases} 0, & s \le |x| \\ \frac{4H_1}{3}\left(1 - \frac{x^2}{s^2}\right), & \frac{s}{2} \le |x| \le s \\ H_1 + H_2, & -\frac{s}{2} \le x \le 0 \end{cases}$$

IV

$$h(x) = \begin{cases} 0, & s \le |x| \\ H_1 + H_2\left(1 + \frac{2x}{s}\right), & -s \le x \le 0 \\ H_1 + H_2\left(1 - \frac{2x}{s}\right), & 0 \le x \le s \end{cases}$$

V

$$h(x) = \begin{cases} 0, & s \le |x| \\ \frac{2H_1}{s}(s - x), & \frac{s}{2} \le |x| \le s \\ \frac{2H_1}{s}(s + x), & -s \le x \le -\frac{s}{2} \\ H_1 + H_2\left(1 - \frac{4x^2}{s^2}\right), & |x| \le \frac{s}{2} \end{cases}$$

VI

4 Derivation of Dispersion Equation

4.1 Solution for inhomogeneous viscoelastic layer

The motion of particles of inhomogeneous viscoelastic layer caused by SH-wave, which is propagating in the *x*-direction and producing displacement in the *y*-direction, is represented by Biot [25] as

$$\frac{\partial}{\partial x} S_{xy} + \frac{\partial}{\partial z} S_{yz} = \rho \frac{\partial^2 v}{\partial t^2} \tag{2}$$

where $S_{xy} = (\mu + v\frac{\partial}{\partial t})\frac{\partial v}{\partial x}$ and $S_{yz} = (\mu + v\frac{\partial}{\partial t})\frac{\partial v}{\partial z}$ are the shear stresses. And ρ, μ and v are the density, elastic, viscosity parameters of the earth's crustal layer.

By using the above stress-displacement relationships, equation (2) reduces to

$$\left(\mu + v\frac{\partial}{\partial t}\right)\frac{\partial^2 v}{\partial x^2} + \frac{\partial}{\partial z}\left(\mu + v\frac{\partial}{\partial t}\right)\frac{\partial v}{\partial z} = \rho\frac{\partial^2 v}{\partial t^2} \tag{3}$$

By using separation of variables method, we assume that

$$v = V(z)e^{i(\omega t - kx)} \tag{4}$$

Equation (3) reduces to

$$\frac{d^2V}{dz^2} + \frac{1}{P}\frac{dP}{dz}\frac{dV}{dz} + \left(\frac{\omega^2\rho}{P} - k^2\right)V = 0 \tag{5}$$

where $P = \mu + i\omega v$ and $i = \sqrt{-1}$.

Assuming the variations in rigidity (μ), viscosity (v) and density (ρ) of the upper layer as the functions of depth $\mu = \mu_0(1 - az)e^{dz}$, $v = v_0(1 - bz)e^{dz}$, $\rho = \rho_0 e^{dz}$. Where μ_0 , v_0 and ρ_0 are the values of rigidity, viscosity and density respectively at the regular interface of layer and half-space. And a, b, d are the real inhomogeneity parameters having dimensions of the inverse of length, associated with rigidity, viscosity and density of viscoelastic layer.

On applying above variations, equation (5) reduces to

$$\frac{d^2V}{dz^2} + \left(\frac{-a_2}{a_1 - a_2 z} + d\right)\frac{dV}{dz} + k^2\left(\frac{c^2}{c_0^2(a_1 - a_2 z)} - 1\right)V = 0 \tag{6}$$

where $c_0 = \sqrt{\frac{\mu_0}{\rho_0}}$, is the velocity of the shear wave of a homogeneous isotropic elastic medium, whose density is ρ_0 and modulus of rigidity is μ_0.

Solution of equation (6) is

$$V(z) = e^{a_4 z}\{c_1 U(a_5, 1, a_6 + a_3 z) + c_2 L(-a_5, a_6 + a_3 z)\} \tag{7}$$

where $U(\alpha, \beta, z)$ is the Hypergeometric function and $L(\alpha, \beta, z)$ is the Laguerre function. From equation (4), the displacement equation for viscoelastic layer is given by

$$v(z) = e^{a_4 z}\{c_1 U(a_5, 1, a_6 + a_3 z) + c_2 L(-a_5, a_6 + a_3 z)\}e^{i(\omega t - kx)} \tag{8}$$

where c_1 and c_2 are arbitrary constants and expressions for a_1, a_2, a_3, a_4, a_5 and a_6 are given in appendix.

4.2 Solution for half-space

The equation of motion for half-space under gravity as given by Biot [25] is

$$\frac{\partial S_{xy}}{} + \frac{\partial S_{yy}}{} + \frac{\partial S_{yz}}{} \qquad \frac{\partial \omega_{yz}}{} \qquad \frac{\partial \omega_{xy}}{} \qquad \frac{\partial^2 v}{}$$

$$\frac{\partial x}{\partial z} - \rho g z \omega_{yz} - \rho g z \frac{\partial y}{\partial z} + \rho g z \frac{\partial x}{\partial x} = \rho \frac{\partial}{\partial t^2} \tag{9}$$

The stress-strain relationship is given by

$$S_{xy} = \lambda e\delta_{xy} + 2\mu e_{xy}$$

and $e = \frac{\partial u}{\partial x} + \frac{\partial v}{\partial y} + \frac{\partial w}{\partial z}$, $\omega_{xy} = \frac{1}{2}\left(\frac{\partial u}{\partial y} - \frac{\partial v}{\partial x}\right)$, $e_{xy} = \frac{1}{2}\left(\frac{\partial u}{\partial y} + \frac{\partial v}{\partial x}\right)$

where λ , μ are rigidity constants of half-space. δ_{xy} and e are the Kronecker delta and the cubical dilatation of the medium.

On using above relations, equation (9) reduces to

$$\left(\mu - \rho g\frac{z}{2}\right)\left(\frac{\partial^2 v}{\partial x^2} + \frac{\partial^2 v}{\partial z^2}\right) + \left(\frac{\partial \mu}{\partial z} - \frac{\rho g}{2}\frac{\partial v}{\partial z}\right) = \rho\frac{\partial^2 v}{\partial t^2} \tag{10}$$

The solution of equation (10) may be assumed as

$$v = V(z)e^{i(\omega t - kx)} \tag{11}$$

On substituting (11) in (10), we get

$$\frac{d^2V}{dz^2} + \frac{\frac{\partial \mu}{\partial z} - \frac{\rho g}{2}}{\mu - \rho g\frac{z}{2}}\frac{dV}{dz} + k^2\left(\frac{\rho c^2}{\mu - \rho g\frac{z}{2}} - 1\right)V = 0 \tag{12}$$

Assuming, the rigidity and the density of the half space as

$$\mu = \mu_1(1 - lz)e^{mz}, \quad \rho = \rho_1 e^{mz}$$

where l and m are real numbers having dimensions of inverse of length. On implementing above variations, equation (12) reduces to

$$\frac{d^2V}{dz^2} + \frac{-l_1 + m - lmz}{1 - l_1 z}\frac{dV}{dz} + k^2\left(\frac{c^2}{c_1^2(1 - l_1 z)} - 1\right)V = 0 \tag{13}$$

Solution of equation (13) is given by

$$V(z) = e^{-l_3 z}\left(c_3 U(l_4, l_5, l_6 + l_7 z) + c_4 L(-l_4, l_5 - 1, l_6 + l_7 z)\right) \tag{14}$$

Ongoing towards the center of earth, the displacement caused by propagating wave vanishes. i.e. $v(z) \to 0$ as $z \to \infty$ therefore,

$$V(z) = c_3 e^{-l_3 z} U(l_4, l_5, l_6 + l_7 z) \tag{15}$$

From equation (10), the displacement of particles in half-space is

$$V(z) = c_3 e^{-l_3 z} U(l_4, l_5, l_6 + l_7 z)e^{i(\omega t - kx)} \tag{16}$$

where c_3 is arbitrary constant and expressions for l_3, l_4, l_5, l_6 and l_7 are given in appendix.

5 Boundary Conditions and Dispersion Equation

(i) The stress is vanishing at free surface $z = -H$, therefore

$$\left(\mu + v\frac{\partial}{\partial t}\right)\frac{\partial v_0}{\partial z} = 0, \quad z = -H$$

(ii) The continuity of the displacement at$z = sh(x)$ requires that

$$v_0 = v_1, \;\; z = sh(x)$$

(iii) The continuity of stress at $z = sh(x)$ requires that

$$\left(\mu + \nu \frac{\partial}{\partial t}\right)\left(\frac{\partial v_0}{\partial z} - s\frac{dh}{dx}\frac{\partial v}{\partial x}\right) = \mu\left(\frac{\partial v}{\partial z} - s\frac{dh}{dx}\frac{\partial v}{\partial x}\right), \quad z = sh(x)$$

Using boundary condition (i)-(iii), we have

$$\begin{aligned} &c_1(-a_4U(a_5, 1, a_6 - a_3H) - a_3a_5U(1 + a_5, 2, a_6 - a_3H)) + \\ &c_2(-a_4L(-a_5, a_6 - a_3H) - a_3L(-1 - a_5, 1, a_6 - a_3H)) = 0 \end{aligned} \tag{17}$$

$$e^{-a_4sh}(c_1U(a_5, 1, a_6 + a_3sh) + c_2L(-a_5, a_6 + a_3sh)) - c_3e^{-l_3sh}U(l_4, l_5, l_6 + l_7sh) = 0 \tag{18}$$

$$\begin{aligned} &c_1(1+q)e^{-a_4sh}[(-a_4 + iskh^j)U(a_5, 1, a_6 + a_3sh) - a_3a_5U(1 + a_5, 2, a_6 + a_3sh)] + \\ &c_2(1+q)e^{-a_4sh}[(-a_4 + iskh^j)L(-a_5, a_6 + a_3sh) - a_3L(-1 - a_5, 1, a_6 + a_3sh)] - \\ &c_3\frac{\mu_1}{\mu_0}e^{-l_3sh}[(-l_3 + iskh^j)U(l_4, l_5, l_6 + l_7sh) - l_7U(1 + l_4, 1 + l_5, l_6 + l_7sh)] = 0 \end{aligned} \tag{19}$$

For a non-zero solution of system of equations (17)–(19), we must have

$$\begin{vmatrix} a_{11} & a_{12} & 0 \\ a_{21} & a_{22} & a_{23} \\ a_{31} & a_{32} & a_{33} \end{vmatrix} = 0 \tag{20}$$

Equation (20) gives the dispersion equation of SH-wave in heterogeneous viscoelastic earth crust lying over an inhomogeneous semi-infinite substratum.

(The expressions for $a_{11}, a_{12}, a_{21}, a_{22}, a_{23}, a_{31}, a_{32}, a_{33}$ are given in appendix.)

5.1 Special Case

When inhomogeneity and viscosity parameters vanish ($a = b = d = l = m = 0$, $\nu_0 = 0$), and the interface becomes flat ($h(x) = 0$), then equation (20) reduces to classical Love wave equation [26].

$$\tan\left(kH\sqrt{\frac{c^2}{c_2^2} - 1}\right) = \frac{\mu_1}{\mu_0}\sqrt{\frac{1 - \frac{c^2}{c_1^2}}{\frac{c^2}{c_0^2} - 1}}$$

6 Numerical Calculation and Discussion

To illustrate the impact of irregular interfaces and the inhomogeneities on SH-wave propagation, numerical simulation has been performed for equation (20). The graphs have been plotted for non-dimensional phase velocity $\frac{c^2}{c_0^2}$ against non-dimensional inhomogeneity parameters such as aH, bH, dH, lH and mH. In order to plot the graphs following numerical values have been used (Gubbins [27]).

Layer: $\mu_0 = 6.02 \times 10^{10} N/m^2$, $\rho_0 = 3364 Kg/m^3$, $\frac{\mu_0}{\nu_0} = 10s^{-1}$

Half-Space: $\mu_1 = 7.45 \times 10^{10} N/m^2$, $\rho_1 = 3293 Kg/m^3$, $\frac{\rho_1 g}{2\mu_1} = 0.5$

For figure no. 2, 3 and 4: $bH = 0.5$, $dH = 1$, $lH = 1$, $mH = 0.4$

For figure no. 5, 6 and 7: $aH = 0.5$, $dH = 1$, $lH = 1$, $mH = 0.4$

For figure no. 8, 9 and 10: $aH = 0.5$, $bH = 1$, $lH = 1$, $mH = 0.4$

For figure no. 11, 12 and 13: $aH = 0.5$, $bH = 0.5$, $dH = 1$, $mH = 0.4$

For figure no. 14, 15 and 16: $aH = 0.5$, $bH = 0.5$, $dH = 1$, $lH = 0.4$

Also, for all graphical presentations the values of kH and s have been taken as 0.5 and 1 throughout the paper.

As the curves are identical for positive and negative x-axis due to the symmetry of imperfect interfaces about z-axis, therefore positive x-axis has been considered for graphical illustrations. This is to be noted that there are 6 different types of irregularities shown in figure no. 1, in which irregularity type I and II, irregularity type III and IV and irregularity type V and VI are just exchange of shapes upside down.

For figure no. 2, 3 and 4, graphs have been plotted for phase velocity against inhomogeneity parameter aH. In figure no. 2, It has been observed that the curves are monotonically increasing for positive values of aH, while it is monotonically decreasing for negative values of aH. At a particular value of aH, the velocity drops down as we move away from the origin towards the direction of wave propagation. At $aH = 0$, the inhomogeneity in the rigidity of the crustal layer is only due to the presence of the exponential function, leading to higher curvature with remarkable influence. It has also been noticed that the magnitude of the velocity is asymmetric or left most skewed due to the contribution of exponential inhomogeneity. Figure no. 3 and 4 have been plotted for the same cause as figure 2, except the fact that it is plotted for irregularity type III and IV and irregularity type V and VI. However, it can be easily noticed that the bunch of curves is shuffled due to the change in the shape of irregularities as per their influences and the coordinates.

Similarly, figure no. 5, 6 and 7 show the impact of bH. Due to the abnormal behavior of wave front near $bH = 0$, only positive real values of bH have been considered. The figures are self-explanatory to differentiate the fluctuation for different sets of irregularities. The pattern being uniform throughout shows that the influences are similar, but velocities are numerically diverted.

The influence of the parameter dH associated with density, rigidity and viscosity on the phase velocity of the SH-wave is depicted by the figures no. 8, 9 and 10. The curves follow the same trend in all the three figures. However, the consistent shifting of curves has been observed in all three figures as the shape of irregularity has been swapped. It also has been found that the phase velocity decreases as the value of dH increases from -1 to 0. While the effect is reversed when dH varies from 0 to 1.

Figure no. 11, 12 and 13 reflect the effect of the inhomogeneity parameter lH involved in the rigidity of half-space. As the horizontal axis of lH increases from -1.5 to 1.5, the velocity decreases consistently. One can also notice that as the rigidity of the half-space decreases, the velocity of the wave also decreases. Unlike previous figures, the slope of the curves are negative throughout, thereby showing a significant effect of irregularity and inhomogeneity.

Keeping the same fashion intact, figures no. 14, 15 and 16 have been plotted to show the influence of parameter mH. It has been observed that the phase velocity decreases gradually and at a slow rate as compared to all the above figures.

The effect of irregularities of the interface on the phase velocity of SH-wave is examined by comparing curves 1-6 associated with interfaces I-VI in figures 2-16, it is observed that as the depth of irregularity along z-axis is increased, the velocity of wave is also increased for any particular value of each parameter(aH, bH, dH, lH, mH) associated with rigidity, viscosity and density of crustal layer and half-space.

7 Conclusion

The transmission of SH-wave in heterogeneous viscoelastic earth's crustal layer with irregular surface lying over heterogeneous half-space has been investigated analytically. The closed form of the dispersion equation has been obtained. Following points have been concluded based on the influence of the irregularities and inhomogeneities of the crustal layer and half-space.

1. The velocity of the SH-wave increases rapidly, as we increase the magnitude of the rigidity of the layer. Which is in accordance with the law that velocity of the shear waves is directly proportional to the rigidity of the material.

2. The phase velocity of SH-wave decreases as the viscosity of the crustal layer increases, which follows the viscosity law.

3. The phase velocity of SH-wave decreases on decreasing the magnitude of the rigidity of half-space.

4. It can also be concluded that the phase velocity of SH-wave is inversely proportional to the density of half-space.

5. The dependence of velocity on the functions that govern the irregularity of the interface has been shown. It has been found that the penetration of SH-wave fluctuates as it passes through the different geometrical regions. The velocity of the wave is affected not only by the depth of the irregularity but also depends on the geometry of the irregular interface of the layer and half-space.

This finding is unique and fills the gap in the existing literature. Although the corrugation in the interface may not exist exactly the same as it appears in the paper, but it may be helpful to explore about crustal and sub-crustal regions of the earth where the interfaces are likely to vary according to the geometry presented here. The above results can be of great importance for geophysical applications in the propagation of SH-wave in the earth's crust with an irregular surface. It can be helpful in predicting geophysical parameters of the earth's core through seismic data analysis and signal processing.

8 Acknowledgment

Authors extend their sincere thanks to SERB-DST, New Delhi for providing financial support under Early Career Research Award with Ref. no. ECR/2017/001185. Authors are also thankful for providing DST-FIST grant with Ref. no. 337 to Department of Mathematics, BITS-Pilani, Hyderabad campus.

9 References

1. Cooper, H. F.: Reflection and transmission of oblique plane waves at an interface between viscoelastic media. Journal of the Acoustical Society of America **42**, 1064–1069 (1967).

2. Shaw, R. P., Bugl, P.: The transmission of plane waves through layered linear viscoelastic media. Journal of the Acoustical Society of America **46**(3B), 649–654 (1969).

3. Bhattacharya, S. N.: Exact solution of SH-wave equation for inhomogeneous media. Bulletin of the Seismological Society of America **60**(6), 1847–1859 (1970).

4. Schoenberg, M.: Transmission and reflection of plane waves at an elastic–viscoelastic interface. Geophysical Journal International **25**, 35–47 (1971).

5. Borcherdt, R. D.: Viscoelastic Waves in Layered Media. Cambridge University Press, New York (2009).

6. Lockett, F. J.: The reflections and refractions of waves at an interface between visco-elastic materials. Journal of the Mechanics and Physics of Solids **10**, 53 (1962).

7. Gogna, M. L., Chander, S.: Reflection and transmission of SH-waves at an interface between anisotropic inhomogeneous elastic and viscoelastic half-spaces. Acta Geologica Polonica **33**(4), 357–375 (1985).

8. Kanai, K.: The effect of solid viscosity of surface layer on the earthquake movements. Bulletin of the Earthquake Research Institute **28**, 31 (1950).

9. Cerveny, V.: Inhomogeneous harmonic plane waves in viscoelastic anisotropic media. Studia Geophysica **48**,

167–186 (2004).
10. Wang, C. D., Wang, W. J., Lin, Y. T., Ruan, Z. W.: Wave propagation in an inhomogeneous transversely isotropic material obeying the generalized power law model. Archive of Applied Mechanics **82**, 919–936 (2012).
11. Guoquan, N., Jinxi, L., Xueqian, F., Zijun, A.: Shear horizontal (SH) waves propagating in piezoelectric–piezomagnetic bilayer system with an imperfect interface. Acta Mechanica **223**, 1999–2009 (2012).
12. Tomar, S. K., Kaur, J.: SH-waves at a corrugated interface between a dry sandy half-space and an anisotropic elastic half-space. Acta Mechanica **190**, 1–28 (2007)
13. Chattopadhyay, A., Gupta, S., Sharma, V., Kumari, P.: Reflection and refraction of plane quasi-P waves at a corrugated interface between distinct triclinic elastic half spaces. International Journal of Solids and Structures **46**(17), 3241-3256 (2009).
14. Vishwakarma, S. K., Gupta, S., Verma, A. K.: Torsional wave propagation in Earth's crustal layer under the influence of imperfect interface. Journal of Vibration and Control **20**(3) 355—369 (2014).
15. Bullen, K. E.: The problem of the earth's density variation. Bulletin of the Seismological Society of America **30**(3), 235–250 (1965).
16. Sari, C., Salk, M.: Analysis of gravity anomalies with hyperbolic density contrast: An application to the gravity data of western Anatolia. Journal of the Balkan Geophysical Society **5**(3), 87–96 (2002).
17. Dey, S.,Mukherjee, S. P.: Love waves in granular medium over a half-space under gravity.Journal of the Acoustical Society of America **72**(5), 1626–1630 (1982).
18. Singh, A. K., Kumar, S., Chattopadhyay, A.: Propagation of torsional waves in a fiber composite layer lying over an initially stressed viscoelastic half-space. International Journal of Geomechanics **16**(1) (2016).
19. Sahu, S. A., Saroj, P. K., Paswan, B.: Shear waves in a heterogeneous fiber-reinforced layer over a half-space under gravity. International Journal of Geomechanics **15**(2) (2015).
20. Chattopadhyay, A., Gupta, S., Singh, A. K., Sahu, S. A.: Propagation of shear waves in an irregular magnetoelastic monoclinic layer sandwiched between two isotropic half-spaces. International Journal of Engineering, Science and Technology **1**(1), 228–244 (2009).
21. Vishwakarma, S. K., Panigrahi, T. R., Kaur, R.: SH-wave propagation in linearly varying fiber-reinforced viscoelastic composite structure uninitial stress. Arabian Journal of Geosciences **12**(2), 12:59 (2019).
22. Fang, X. Q., Zhang, T. F., Li, H. Y.: Elastic-slip interface effect on dynamic response of a lined tunnel in a semi-infinite alluvial valley under SH waves. Tunnelling and Underground Space Technology, **74**, 96–106 (2018).
23. Li, B. L., Fang, X. Q., Yuan, R. J.: Predicting the crack open displacements of a partially debonded pipeline in rock mass under SH waves. Engineering Failure Analysis. **96**, 80–87 (2019).
24. Campillo, M.: Modelling of SH-wave propagation in an irregularly layered medium-application to seismic profiles near a dome.Geophysical Prospecting, **35**(3), 236—249 (1987).
25. Biot, M. A.: Mechanics of Incremental Deformation, John Willey and Sons, New York (1965).
26. Love, A. E. H.: Some Problems of Geo-dynamics, Cambridge University Press, London (1911).
27. Gubbins, D.: Seismology and Plate Tectonics, Cambridge University Press, Cambridge (1990).

10 Appendix

$q = i\omega \frac{\eta_0}{\mu_0}$ where $\omega = ck$

$a_1 = 1 + q$

$$a_2 = a + qb$$

$$a_3 = \sqrt{d^2 + 4k^2}$$

$$a_4 = \frac{d+a_3}{2}$$

$$a_5 = \frac{a_2(d_3)+2k^2c^2/c^2}{2a_2a_3}_0$$

$$a_6 = \frac{-a_1a_3}{a_2}$$

$$l_1 = l + \frac{g\rho_1}{2\mu_1}$$

$$l = \sqrt{\frac{2\mu_1 2}{1} \quad 2\ 2}$$

$$l_3 = \frac{-lm+l_2}{4k\sqrt{l\ 24+\ l\ 2}}m$$

$$l_4 = (ll_1^2m + l^2m^2 - ll_1m^2 + l^2l_2 - lml_2 + l_1ml_2 + 2c_{01}k^2l^2(c/c_0)^2)/2l^2l_2$$

$$l_5 = 1 + \frac{(l-l_1)m}{l_1^2}$$

$$l_6 = \frac{-l_2}{l_1^2}$$

$$l_7 = \frac{l_2}{l_1}$$

$$a_{11} = -a_4U\,(a_5,\,1,\,a_6 - a_3H) - a_3a_5U\,(1 + a_5,\,2,\,a_6 - a_3H)$$

$$a_{12} = -a_4L(-a_5,\,a_6 - a_3H) - a_3L(-1 - a_5,\,1,\,a_6 - a_3H)$$

$$a_{21} = e^{-a_4sh}U\,(a_5,\,1,\,a_6 + a_3sh)$$

$$a_{22} = e^{-a_4sh}L(-a_5,\,a_6 + a_3sh)$$

$$a_{23} = -e^{-l_3sh}U(l_4, l_5, l_6 + l_7sh)$$

$$a_{31} = (1+q)e^{-a_4sh}\,[(-a_4 + iskh^j)U(a_5, 1, a_6 + a_3sh) - a_3a_5U(1 + a_5, 2, a_6 + a_3sh)]$$

$$a_{32} = (1+q)e^{-a_4sh}\,[(-a_4 + iskh^j)L(-a_5,\,a_6 + a_3sh) - a_3L(-1 - a_5,\,1,\,a_6 + a_3sh)]$$

$$a_{33} = -\frac{\mu_1}{\mu_0}e^{-l_3sh}\,[(-l_3 + iskh^j)U(l_4, l_5, l_6 + l_7sh) - l_4l_7U(1 + l_4, 1 + l_5, l_6 + l_7sh)]$$

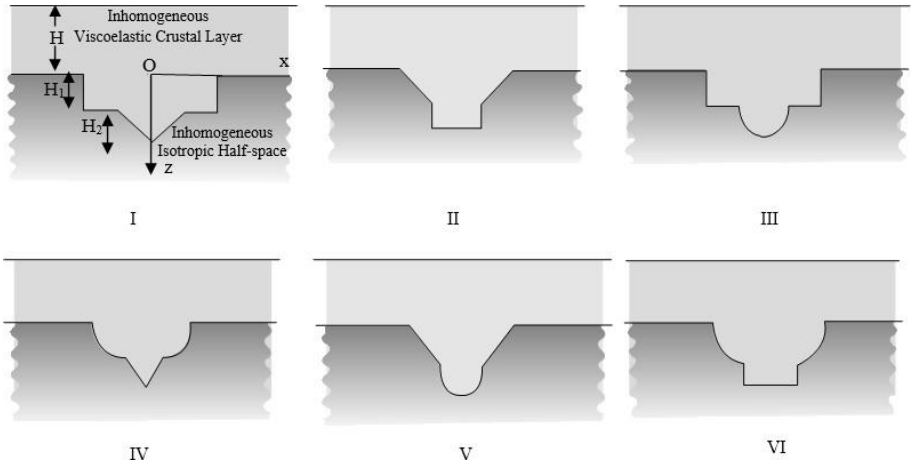

Figure 1: Geometry of problem with 6 different types of irregular interfaces.

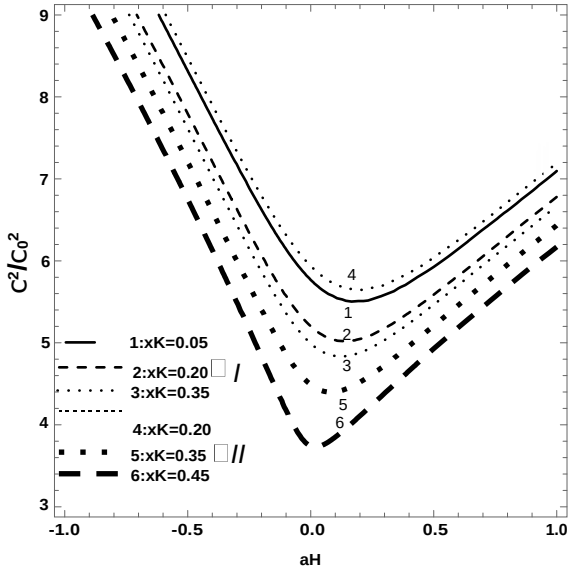

Figure 2: Dimensionless phase velocity against dimensionless *aH* for irregularity type I and II .

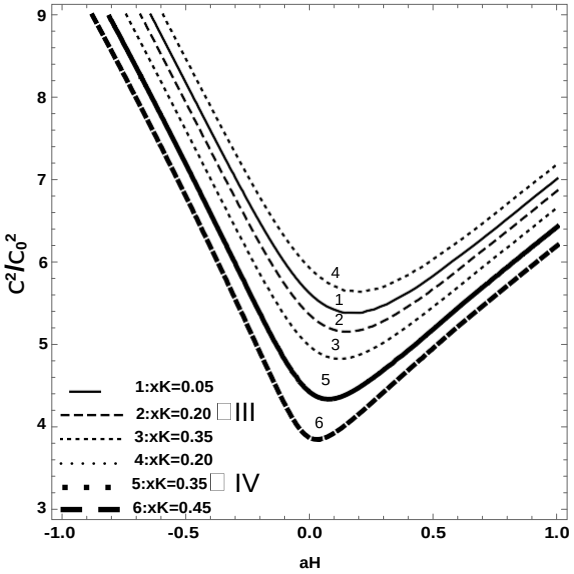

Figure 3: Dimensionless phase velocity against dimensionless *aH* for irregularity type III and IV .

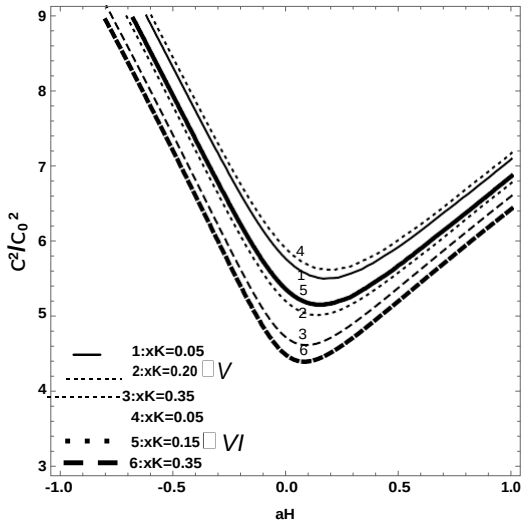

Figure 4: Dimensionless phase velocity against dimensionless *aH* for irregularity type V and VI .

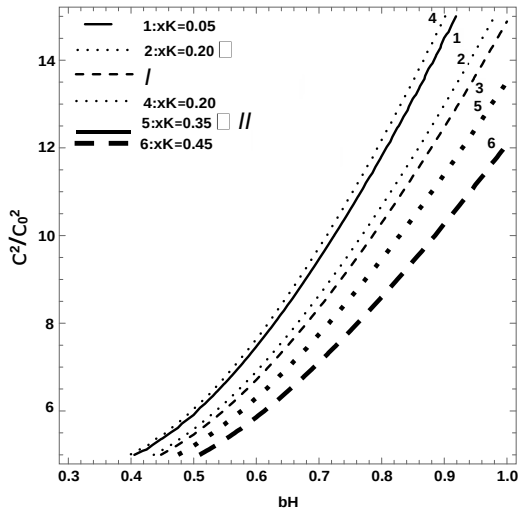

Figure 5: Dimensionless phase velocity against dimensionless *bH* for for irregularity type I and II .

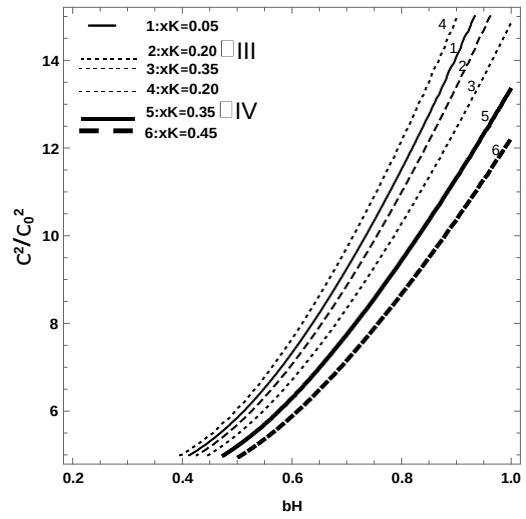

Figure 6: Dimensionless phase velocity against dimensionless *bH* for irregularity type III and IV .

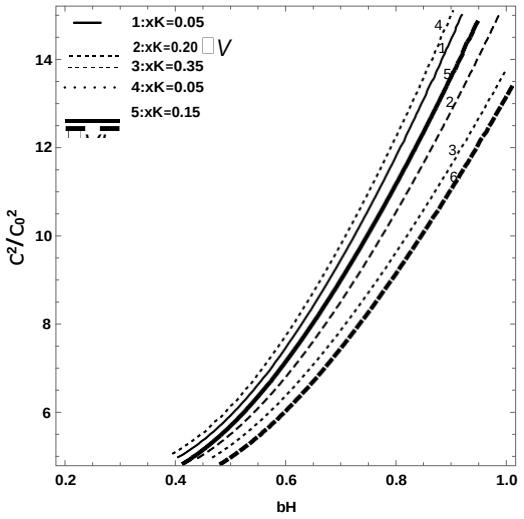

Figure 7: Dimensionless phase velocity against dimensionless *bH* for for irregularity type V and VI .

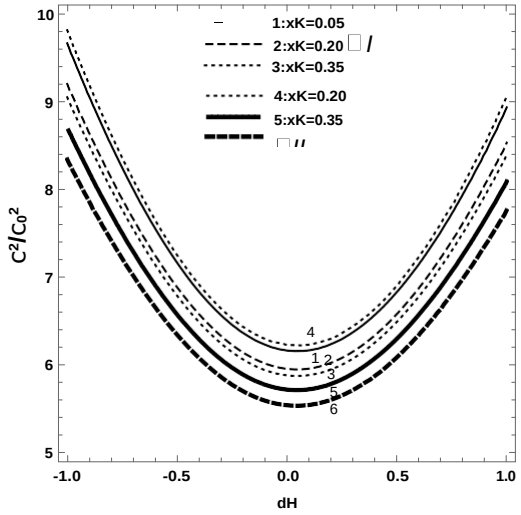

Figure 8: Dimensionless phase velocity against dimensionless *dH* for for irregularity type I and II .

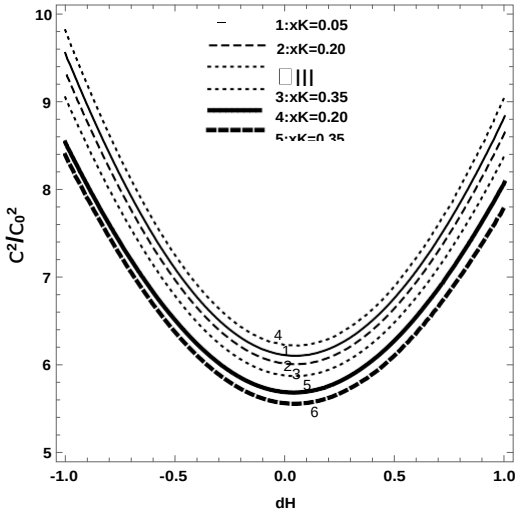

Figure 9: Dimensionless phase velocity against dimensionless *dH* for irregularity type III and IV .

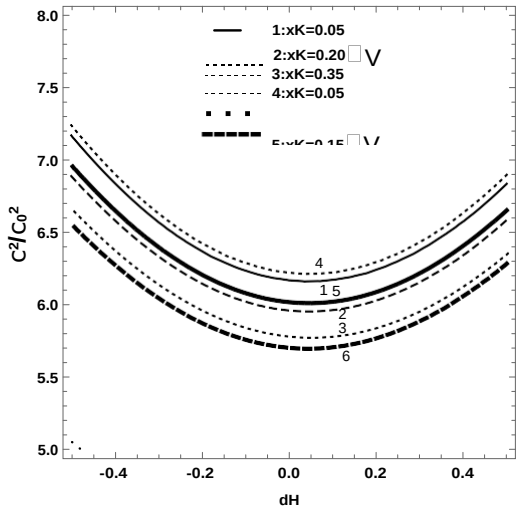

Figure 10: Dimensionless phase velocity against dimensionless *dH* for for irregularity type V and VI .

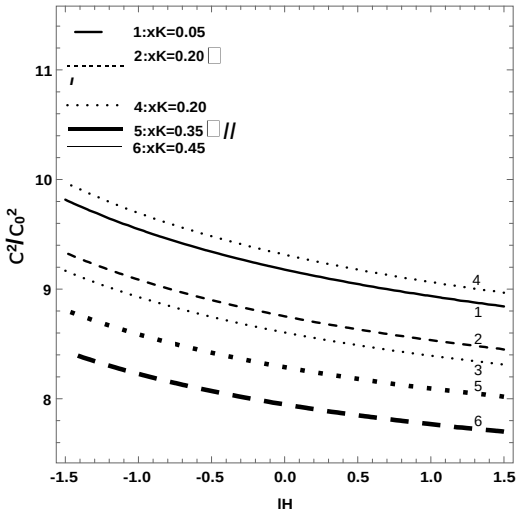

Figure 11: Dimensionless phase velocity against dimensionless *lH* for irregularity type I and II .

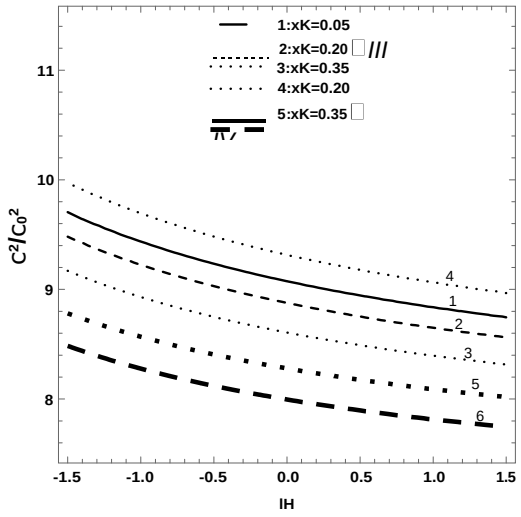

Figure 12: Dimensionless phase velocity against dimensionless *lH* for irregularity type III and IV .

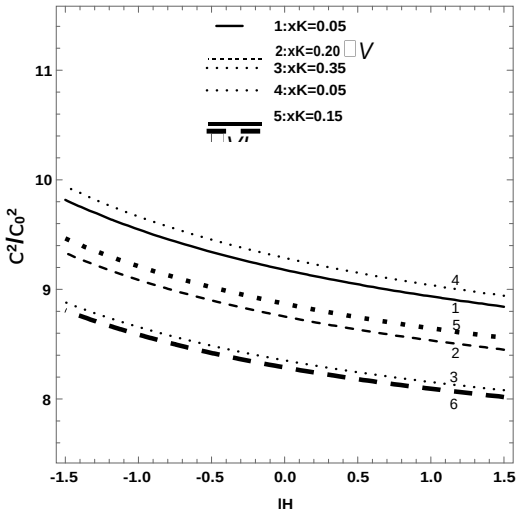

Figure 13: Dimensionless phase velocity against dimensionless *lH* for irregularity type V and VI .

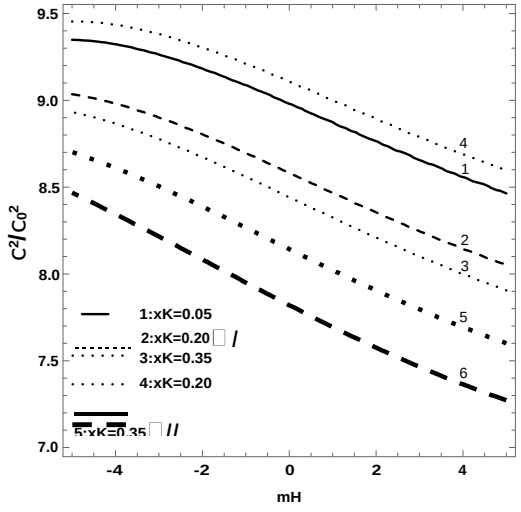

Figure 14: Dimensionless phase velocity against dimensionless *mH* for irregularity type I and II .

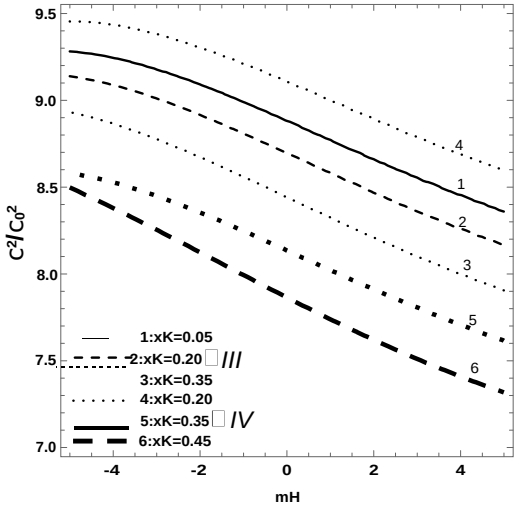

Figure 15: Dimensionless phase velocity against dimensionless *mH* for irregularity type III and IV .

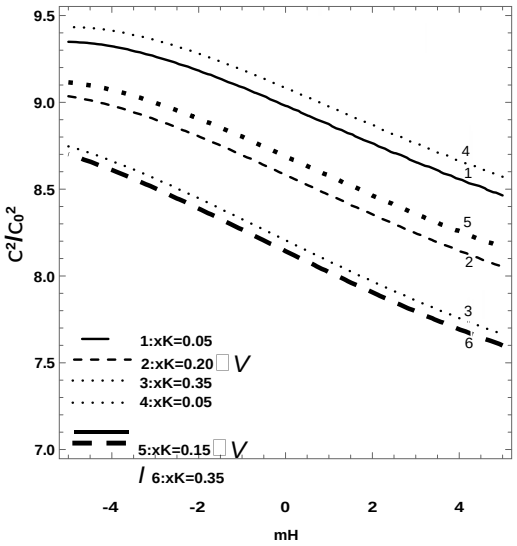

Figure 16: Dimensionless phase velocity against dimensionless *mH* for irregularity type V and VI .